iScience

CellPress
OPEN ACCESS

Article

Phosphorylated YBX2 is stabilized to promote glycolysis in brown adipocytes

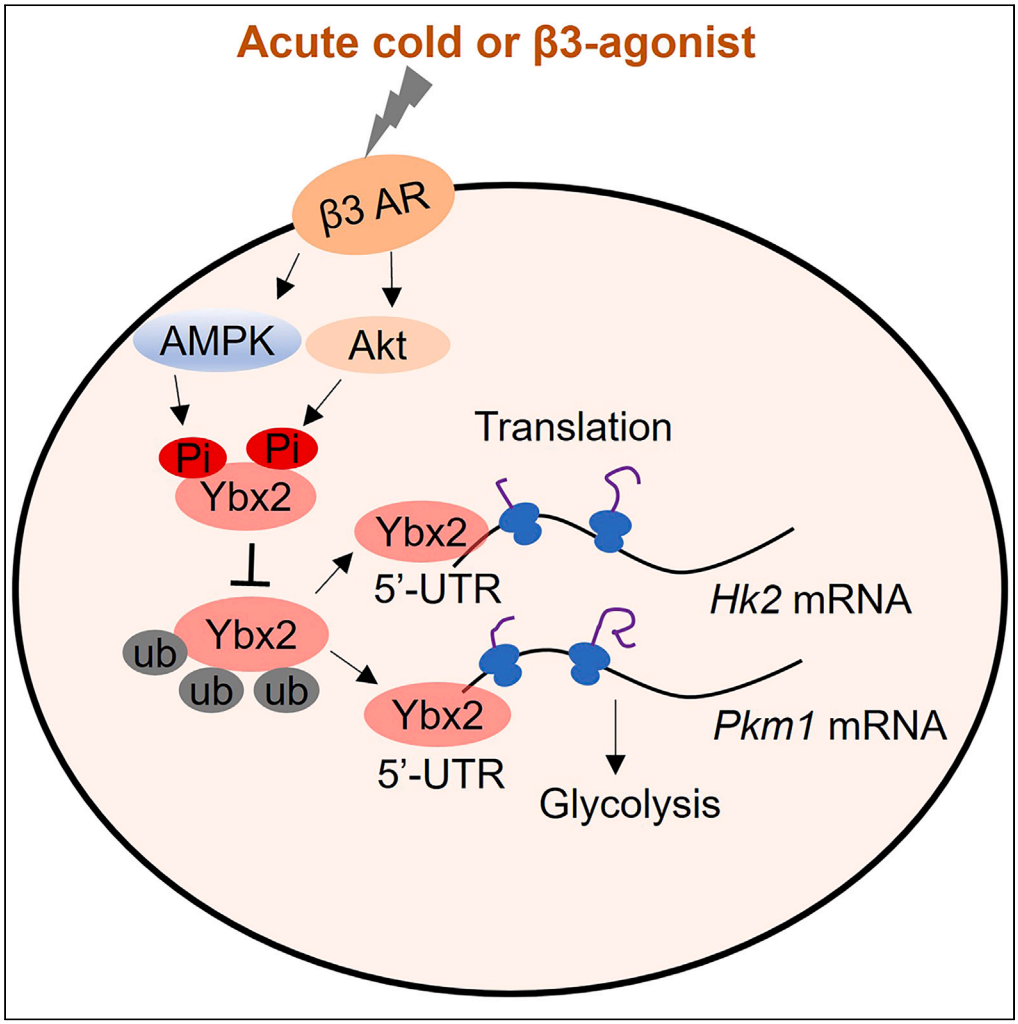

Qingwen Zhao, Chao Yu, Xiaoxuan Xu, ..., Haiyan Huang, Yue Gao, Dongning Pan

gy9821@sina.com (Y.G.)
dongning.pan@fudan.edu.cn (D.P.)

Highlights

AMPK and Akt2 phosphorylate YBX2 at Thr115 and Ser137, respectively

Phosphorylation on YBX2 retards its ubiquintination-mediated degradation

YBX2 promotes translation of glycolytic genes by binding to their 5′-UTR

Zhao et al., iScience *26*, 108091
October 20, 2023 © 2023 The Author(s).
https://doi.org/10.1016/j.isci.2023.108091

iScience

CellPress
OPEN ACCESS

Article

Phosphorylated YBX2 is stabilized to promote glycolysis in brown adipocytes

Qingwen Zhao,[1,2,3] Chao Yu,[1,3] Xiaoxuan Xu,[1] Wenfang Jin,[1] Zhe Zhang,[1] Haiyan Huang,[1] Yue Gao,[2,*] and Dongning Pan[1,4,*]

SUMMARY

Y-box binding protein 2 (YBX2) is an essential modulator of brown adipose tissue activation, yet the regulation on its own expression and the involved mechanism remains largely unknown. Herein, we report the YBX2 protein level, but not mRNA level, is induced in response to acute β-adrenergic signaling. In this context, YBX2 is a dual substrate for both AMPK and Akt2. The phosphorylation at Thr115 by AMPK or at Ser137 by Akt2 facilitates YBX2 accumulation in brown adipocytes by decreasing ubiquitination-mediated degradation. Beyond stabilizing PGC1α mRNA, increased YBX2 upon thermogenic activation assists the expression of glycolytic enzymes, promotes glucose utilization and lactate production. Mechanistically, YBX2 modulates translation of glycolytic genes via direct binding to 5′-UTRs of these genes. Together these findings suggest YBX2 is responsive to thermogenic stimuli by phosphorylation modification, and stabilized YBX2 helps to boost glycolysis and thermogenesis in brown adipocytes.

INTRODUCTION

Obesity has become an epidemic public health problem, leading to an increased morbidity of metabolic disorders such as type 2 diabetes, cardiovascular disease, and some types of cancer. Adipose tissue plays a fundamental role in maintaining systemic energy homeostasis. There are two types of thermogenic adipocytes,[1] namely, classic brown adipocytes and beige adipocytes. Brown adipose tissue (BAT) is enriched with a mass of mitochondria that specifically expresses uncoupling protein 1 (UCP1) to dissipate the mitochondrial proton gradient for heat production. In response to prolonged cold exposure, chronic treatment of β-adrenergic receptor agonist or long-period of exercise, the number of beige adipocytes is distinctly increased, accompanied by enhanced UCP1-dependent or UCP1-independent thermogenesis.[2–5] Since activated thermogenic adipocytes are believed to possess anti-obesity and anti-diabetes potential, they have attracted considerable research interest.

The regulation of adipocyte thermogenic activity is involved in neuronal control, endocrine factors, transcriptional or post-transcriptional circuits. An RNA-binding protein, Y-box binding protein 2 (YBX2), was revealed to regulate adipocyte thermogenesis by stabilizing the *Pgc1α*[6] mRNA. YBX2 is initially known as a germ-cell-specific protein that coordinates the storage and degradation of mRNAs to delay translation during spermiogenesis.[7,8] The whole-body *Ybx2* knockout mice were infertile and cold intolerant with downregulated mitochondrion functions and suppressed fatty acid metabolism in their BATs. Moreover, the transcription of *Ybx2* mRNA was reported to be induced by a 7-day cold challenge in the previous study.[6] Intriguingly, we found 6-h cold exposure had already been able to increase the YBX2 protein level, without altering its mRNA level. Following this clue, we disclose that the stability of YBX2 protein is enhanced by Thr115 and Ser137 phosphorylation modification. In addition to thermogenic regulation, YBX2 promotes the mRNA translation of glycolytic genes by directly binding to their 5′-UTRs, which facilitates brown adipocytes glycolysis in response to β-adrenergic signaling.

RESULTS

The level of YBX2 protein, not mRNA, is regulated by acute thermogenic stimuli

Ybx2 gene initially attracted our attention due to its high expression level in BAT relative to epididymal white fat tissues (eWAT) in our RNA-seq data (Figure S1A).[9] The quantitative PCR and western blot confirmed that *Ybx2* was a BAT-enriched gene (Figures S1B and S1C; the specificity of YBX2 antibody was shown in Figure S1D by knocking down *Ybx2* in brown adipocytes, and the band of YBX2 was near the 50 kDa). Inhibiting expression of YBX2 without disturbance of *Ybx1* and *Ybx3* level decreased the *Ucp1* mRNA and protein level in brown fat cells, consistent with the previous study to show its involvement in thermogenic regulation (Figures S1E and S1F).[6] Knocking down *Ybx1* or

[1]Key Laboratory of Metabolism and Molecular Medicine of the Ministry of Education, Department of Biochemistry and Molecular Biology of School of Basic Medical Sciences, Fudan University, Shanghai 200032, China
[2]Department of Geriatrics, Affiliated Hangzhou First People's Hospital, Zhejiang University School of Medicine, Hangzhou, China
[3]These authors contributed equally
[4]Lead contact
*Correspondence: gy9821@sina.com (Y.G.), dongning.pan@fudan.edu.cn (D.P.)
https://doi.org/10.1016/j.isci.2023.108091

This is an open access article under the CC BY-NC-ND license (http://creativecommons.org/licenses/by-nc-nd/4.0/).

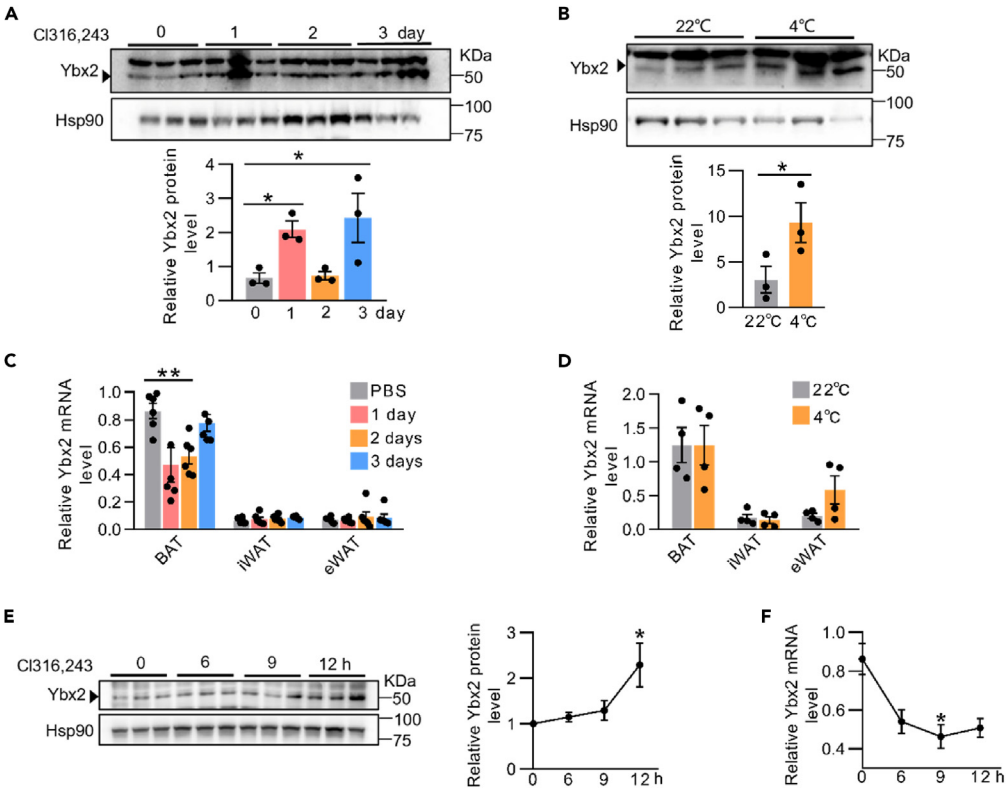

Figure 1. YBX2 protein, not the mRNA, is induced by acute β-adrenergic signaling

(A) YBX2 protein level (top) and protein quantification (bottom) in BAT of mice. C57BL/6J mice were intraperitoneally (i.p.) injected Cl316,243 or phosphate-buffered saline at a dose 0.5 μg/g body weight for 1, 2, or 3 days (n = 3 each group).

(B) Immunoblots for YBX2 protein (top) in BAT after mice were exposed to 4°C for 6 h. Mice housed at room temperature (22°C) were used as controls. Bottom panel showed quantification of YBX2 protein level (n = 3 each group).

(C) *Ybx2* mRNA level in adipose tissues was analyzed by quantitative PCR. Mice were treated as in (A) (n = 6 each group).

(D) *Ybx2* mRNA level in adipose tissues from mice exposed to 4°C for 6 h (n = 4).

(E) YBX2 protein level (left) and protein quantification (right) in brown adipocytes (n = 3 independent cultures). Immortalized brown preadipocytes differentiated into mature adipocytes and were treated by 10 μM Cl316,243 for the indicated time on day 6.

(F) *Ybx2* mRNA level in mature brown adipocytes in (E) (n = 3 independent cultures). Data are expressed as mean ± SEM of biologically independent samples. *p < 0.05, **p < 0.01 by two-tailed unpaired Student's *t* test (for B, D) or one-way ANOVA (for A, C, E, F). See also Figure S1.

Ybx3 did not affect *Ucp1* expression, indicating YBX2 specifically regulates adaptive thermogenesis (Figures S1G and S1H). As a cold-induced gene, the YBX2 protein level was strikingly increased in BAT of mice after 1 or 3-day intraperitoneal injection of β3-adrenergic receptor (β3AR) agonist Cl316,243, or increased 2-fold upon only 6-h cold exposure (Figures 1A and 1B). However, all these managements did not increase *Ybx2* mRNA level (Figures 1C and 1D). The discrepancy between YBX2 protein and mRNA levels was also shown in cultured brown adipocytes that were treated by Cl316,243 for 12 h (Figures 1E and 1F), indicating YBX2 expression is modulated post-transcriptionally by the short-term β-adrenergic activation in adipocytes.

AMPK phosphorylates YBX2 at Thr115 and Ser189

Cold exposure and β3AR agonist enhance the thermogenic capacity of BAT, which is mediated through several signaling pathway, primarily including cAMP-PKA, AMPK, and mTORC2-Akt cascade.[10] All these protein kinase pathways coordinate to bring out a variety of biological effects by phosphorylating specific substrates, which may alter the substrate stability, localization or interacting partners. To figure out whether the observed increase in the YBX2 protein level in response to thermogenic impulse is due to one of the activated signaling pathway, we first verified the activation of these pathways in BAT after acute cold challenges. As Figure 2A showed, cold exposure for 6 h spurred AMPK, Akt, and PKA signaling in BAT, indicated by increased phosphorylation of AMPKα1, Akt2, and PKA substrates (Figure 2A). Similarly, the activation of the AMPK, Akt2, and PKA kinases was also observed in Cl316,243-treated brown adipocytes *in vitro* (Figure S2A). At the same time, YBX2 protein was shown phosphorylation at multiple Ser/Thr sites (including S83, S137, S189, and S208, etc) in Cl316,243-treated brown adipocytes as revealed by the liquid chromatography with tandem mass spectrometry (LC-MS/MS) analysis (Table S1). Then we stimulated the mature brown adipocytes with Cl316,243 simultaneously in the presence of the PKA inhibitor H-89, the AMPK inhibitor compound C, or the

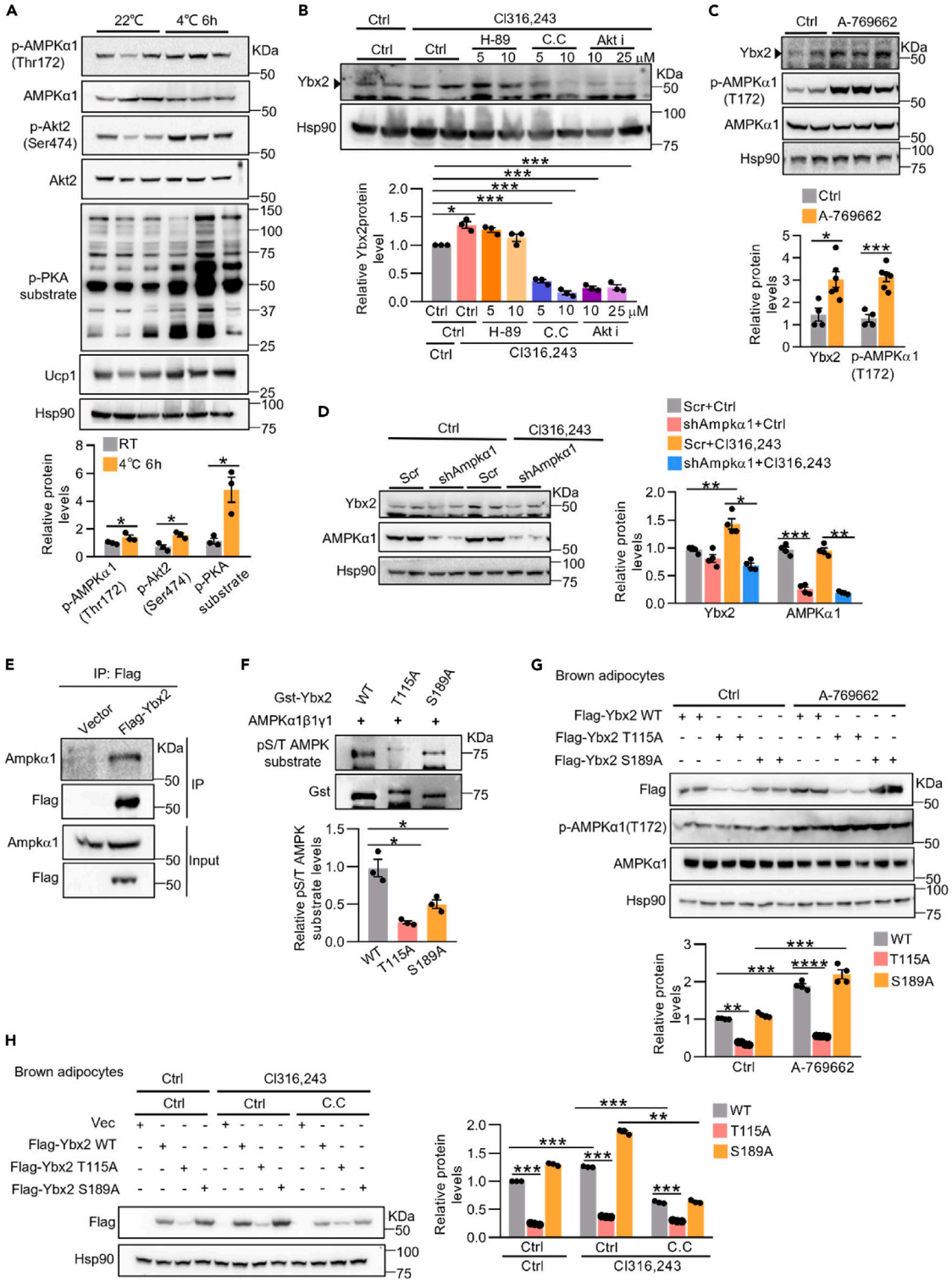

Figure 2. AMPK phosphorylates YBX2 at Thr115 and Ser189

(A) Immunoblot analysis (top) of the indicated proteins in BAT. Mice were housed at 22°C or exposed to 4°C for 6 h (n = 3 each group). Bottom panel showed quantification of protein levels.

(B) Representative YBX2 protein level (top) in differentiated brown adipocytes treated with 10 μM Cl316,243 for 12 h in the presence of H-89, compound C or Akt inhibitor VIII. Quantification of YBX2 protein level was shown in the bottom panel (n = 3 independent cultures).

Figure 2. *Continued*

(C) Representative immunoblot analysis of the indicated proteins in mature brown adipocytes stimulated with A-769662 (10μM) for 12 h. Quantification of protein levels was shown in the bottom panel (n = 4–6 independent cultures).

(D) Representative YBX2 protein level in mature brown adipocytes. Brown adipocytes were infected with sh*AMPKα1* lentivirus on day 2, and treated with 10 μM Cl316,243 for 12 h on day 6. Quantification of protein levels was shown in right panel (n = 4 independent cultures).

(E) Immunoprecipitation of Flag-YBX2 protein followed by western blot to detect AMPKα1 in mature brown adipocytes. The experiment was repeated independently for three times.

(F) Representative phosphorylated AMPK substrate levels in *in vitro* kinase assay. The recombinant GST-YBX2 protein and recombinant AMPKα1β1γ1 kinase were incubated at 30°C for 30 min followed by western blot analysis (top). Three independent experiments were repeated and the quantified phosphorylated substrate levels were shown in bottom panel (n = 3 independent experiments).

(G and H) Representative YBX2 protein level in mature brown adipocytes. Preadipocytes were infected with lentiviruses carrying *YBX2 WT*, *T115A*, or *S189A*, and induced for differentiation. Adipocytes were treated with AMPK agonist A-769662 (5 μm) (G) or compound C (10 μm) (H) in the presence of Cl316,243 (10 μM) for 12 h. Quantification of protein levels was shown in the bottom panel (G, n = 4 independent cultures) or in the right panel (H, n = 3 independent cultures). Data are expressed as mean ± SEM of biologically independent samples. *p < 0.05, **p < 0.01, ***p < 0.001 by two-tailed unpaired Student's *t* test (for A, C), or by one-way ANOVA (for B, D, F), or by two-way ANOVA (for G, H). See also Figure S2.

Akt inhibitor VIII.[11] Cl316,243-induced increase of YBX2 was blocked by compound C or Akt inhibitor, but not by the PKA inhibitor (Figure 2B and S2B-S2D).

To pinpoint whether AMPK signaling is required for YBX2 induction, we supplemented the differentiated brown adipocytes with the AMPK-activator A-769662 or knocked down *Ampkα1*. A-769662 treatment mirrored Cl316,243 agonist to augment YBX2 protein expression (Figure 2C). Instead, transduction of lentivirus *Ampkα1* shRNA to brown fat cells on day 2 blocked Cl316,243-induced YBX2 protein (Figure 2D). We predicted YBX2 could interact with the catalytic subunit of AMPK and be phosphorylated by AMPK. Indeed, immunoprecipitation assay detected the endogenous AMPKα1 in YBX2 immunoprecipitates from brown adipocytes whole-cell extracts that expressed Flag-YBX2, confirming YBX2 and AMPKα1 existed in the same protein complex (Figure 2E). To test whether YBX2 is a substrate of AMPK, *in vitro* kinase assay was performed with the recombinant AMPKα1β1γ1 kinase and purified GST-YBX2 protein following LC-MS/MS analysis (Figure S2E). Among the identified phosphorylation sites in YBX2 protein (Table S2), the amino acid sequence around Thr115 (T115) and Ser189 (S189) conformed to the consensus AMPK substrate motif (Figure S2F). When the T115 and S189 were mutated to alanine in the YBX2 protein, T115A and S189A lost 75% and 50% of the phosphorylated AMPK substrate level, respectively, indicating T115 and S189 were the two dominant phosphorylation sites by AMPK (Figure 2F).

We then investigated the influence of the phosphorylation at T115 or S189 on YBX2 protein level. When the wild type (WT), T115A or S189A YBX2 was introduced into brown adipocytes, the mRNA level of endogenous *Ybx2* was not affected (Figure S2G). We noticed T115A protein level was lower than those of the other two constructs, even though their mRNA levels were similar (Figures 2G and S2H). Furthermore, activation of AMPK by A-769662 compound could not increase T115A expression level, but caused substantial increase of the WT and S189A YBX2 protein (Figure 2G). Accordingly, inhibition of AMPK activity by compound C greatly impaired the Cl316,243-induced expression of the WT and S189A YBX2, without affecting the T115A level (Figure 2H). The responsiveness of YBX2 to AMPK signaling also took place in HEK293T cells (Figures S2I and S2J). Taken together, the data here demonstrates that the T115 and S189 of YBX2 protein can be phosphorylated by AMPK, and T115 phosphorylation enhances YBX2 protein expression. As for S189 phosphorylation, it does not have clear effect on the YBX2 level, and the physiological significance needs to be explored further.

Akt phosphorylates YBX2 at S137

As shown in Figure 2B, Akt inhibitor completely abolished YBX2 induction by Cl316,243 in brown adipocytes, suggesting the potential involvement of Akt kinase in YBX2 phosphorylation and protein level regulation. During the *in vitro* induction of brown preadipocyte differentiation, insulin is always supplemented in cultured media to activate Akt. When we treated the mature brown adipocytes with Akt inhibitor VIII, the level of YBX2 was toned down (Figure 3A). Once we removed insulin from the culture medium for 12 h, the YBX2 protein level and phosphorylated Akt2 level in mature brown adipocytes were dramatically reduced (Figure 3B). An interaction between Akt2 and YBX2 was detected when Flag-Akt2 and HA-YBX2 were co-expressed in HEK293T cells (Figure S3A). Furthermore, ectopically expressed Flag-YBX2 interacted with endogenous Akt2 in brown adipocytes (Figure 3C).

A scan for phosphorylation motifs in YBX2 with PhosphoSitePluswebsite (www.phosphosite.org/homeAction.action) highlighted Ser137 (S137) within the cold shock domain (CSD) as a potential phosphorylation site of the Akt kinase. YBX1 was reported to be phosphorylated at Ser102 previously,[12] the amino acid sequence around which was conserved in YBX2 corresponding to S137 (Figure 3D). Moreover, phosphorylated S137 was present in Cl316,243 treated adipocytes (Table S1). We performed the *in vitro* kinase assay with the purified GST-YBX2 WT, T115A, or S137A and constitutively active Akt (CA-Akt) protein (Figure S3B). As shown in Figure 3E, WT and T115A YBX2 were phosphorylated by CA-Akt, while the S137A mutant abolished phosphorylation level, indicating S137 was a bona fide Akt phosphorylation site (Figure 3E). Then we expressed similar level of Flag-tagged WT or S137A YBX2 in brown adipocytes by lentivirus infection, and the endogenous *Ybx2* mRNA level was not affected (Figures S3C and S3D). The protein level of S137A was lower than that of WT in brown adipocytes supplemented with insulin, and was insensitive to insulin withdrawal (Figure 3F). In addition, the Cl316,243-elicited increase in WT YBX2 level was diminished by Akt inhibitor, but S137A was almost irresponsive to Akt inhibitor (Figure 3G). Similarly, the protein level of WT but not

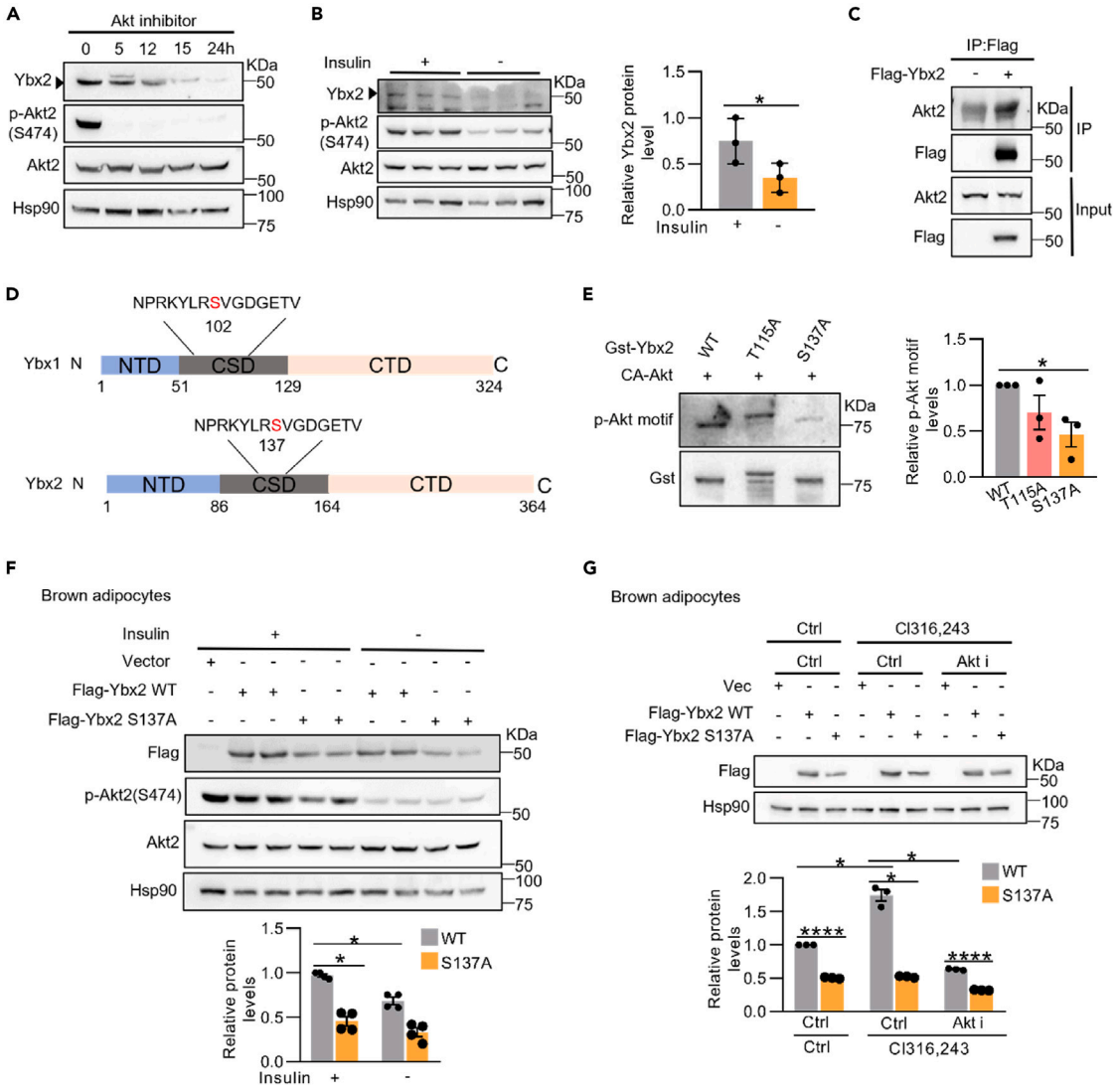

Figure 3. Akt phosphorylates YBX2 at Ser 137

(A) Representative YBX2 protein level in mature brown adipocytes treated with 25 μM Akt inhibitor VIII for the indicated time. The experiment was repeated for three times.

(B) Immunoblot analysis of the indicated protein in brown adipocytes (left) and quantification of the YBX2 protein level (right, n = 3 individual cultures). The culture medium was supplemented with or without insulin for 24 h from day 5 to day 6 of differentiation.

(C) Immunoprecipitation of Flag-YBX2 protein from mature brown adipocytes followed by western blot to detect Akt2. The experiment was repeated for three times.

(D) Alignment of YBX1 and YBX2 amino acid sequence around the potential Akt2 substrate motif.

(E) Representative phosphorylated Akt motif level in YBX2 protein. *In vitro* kinase assay used recombinant GST-YBX2 protein and recombinant constitutive active Akt2 kinase followed by western blot analysis (left). The experiment was repeated for three times and quantification of phosphorylated Akt substrate levels was shown in the right panel (n = 3 independent experiments).

(F) Immunoblot analysis of YBX2 WT and S137A level in mature brown adipocytes. Cultured adipocytes carrying lentiviral YBX2 WT or S137A were incubated in medium with or without insulin for 24 h before immunoblot analysis. Two independent experiments were repeated and quantification of protein levels was shown in the bottom panel (n = 4 independent cultures).

(G) Immunoblot analysis of YBX2 WT and S137A level in mature brown adipocytes. Adipocytes carrying YBX2 WT or S137A were treated with 25 μM Akt inhibitor VIII in the presence of CI316,243 (10 μm) for 12 h before immunoblot analysis. The experiment was repeated for three times and quantification of protein levels was shown in the bottom panel (n = 3 independent experiments). Data are expressed as mean ± SEM of biologically independent samples. *p < 0.05, ***p < 0.0001 by two-tailed unpaired Student's *t* test (for B), or by one-way ANOVA (for E), or by two-way ANOVA (for F, G). See also Figure S3.

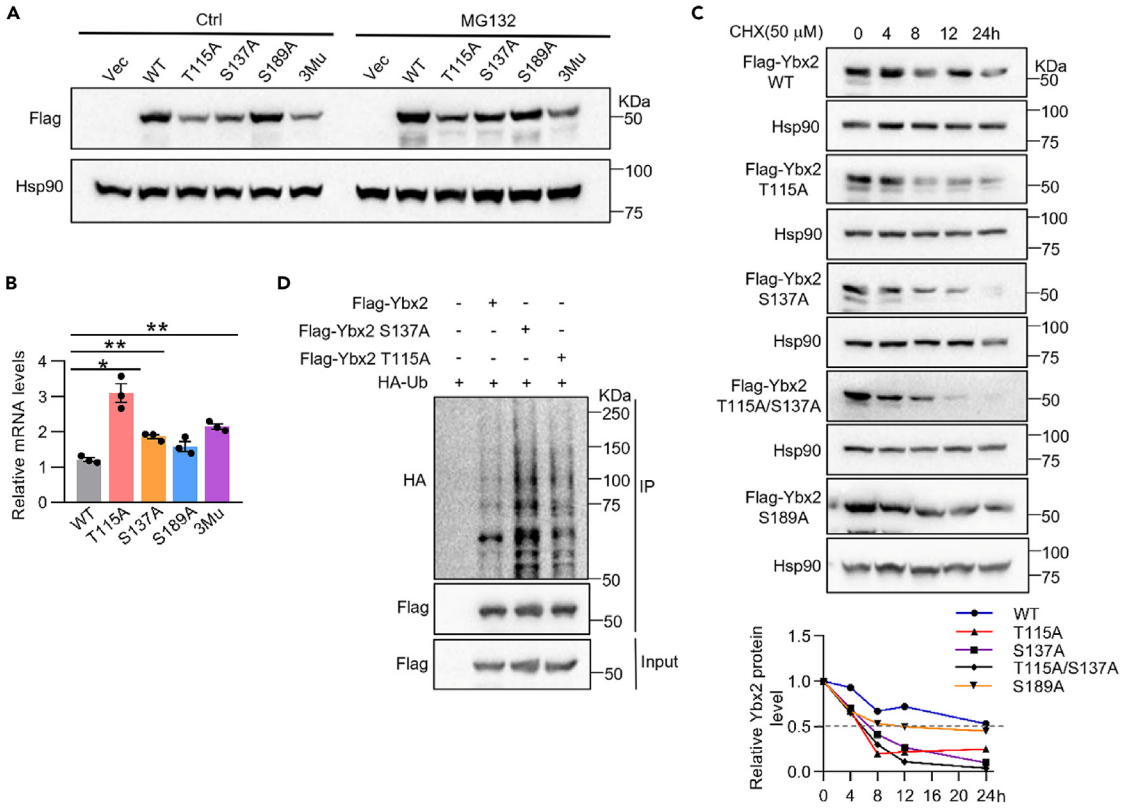

Figure 4. Phosphorylation at Thr115 and Ser137 retards YBX2 degradation

(A) WT or mutant YBX2 protein levels in HEK293T cells. *Ybx2* WT, T115A, S137A, S189A, or 3Mu plasmid was transfected into HEK293T cells. Western blot was performed after 5 μM MG132 treatment for 12 h. The experiment was repeated for three times.

(B) *Ybx2* mRNA level in HEK293T cells with indicated plasmid transfection (n = 3 individual samples).

(C) Cycloheximide chase assay (top) and quantification (bottom) of YBX2 protein level in HEK293T cells. The experiment was repeated for three times.

(D) Western blot detected ubiquitination of YBX2 WT, T115A and S137A protein in HEK293T cells. Flag-YBX2 protein was pulled down and HA antibody detected the ubiquitination level. The experiment was repeated for three times. Data are expressed as mean ± SEM of biologically independent samples. *p < 0.05, **p < 0.01 by one-way ANOVA. See also Figure S4.

S137A YBX2 was regulated by Akt inhibitor or insulin treatment in HEK293T cells (Figures S3E and S3F). These observations indicate that Akt phosphorylating YBX2 at S137 site also contributes to the upregulation of the YBX2 protein level.

Phosphorylation at T115 or S137 retards YBX2 degradation

To further figure out how the phosphorylation of YBX2 increases its protein level, we compared the expression levels of 5 forms of YBX2 (WT, T115A, S137A, S189A, T115A/S137A/S189A referred to as 3Mu) before and after the proteasome inhibitor MG132 treatment in HEK293T cells. Western blot analysis showed that the expression level of WT and S189A was similar. However, the levels of T115A, S137A, and 3Mu were much lower than WT, although the mRNA level of each mutant was not low (Figures 4A and 4B). MG132 partly rescued the decrease of the protein level of T115A, S137A, and 3Mu (Figure 4A), indicating ubiquitination-mediated degradation is responsible for the decreased level of these mutants. We then checked the half-life time of WT, T115A, S137A, T115A/S137A, and S189A. Noticeably, the half-life time of T115A and S137A decreased to 5 to 8 h as compared to 24 h for WT. The T115A/S137A double mutant did not show further decreased half-life time relative to either of the single point mutant, implying phosphorylation on T115 and S137 had no additive effect on YBX2 level. The mutant S189A shortened the half-life time to 12 h by an unknown mechanism (Figure 4C). Consistently, T115A and S137A had markedly increased ubiquitination level (Figure 4D). The observed more ubiquitination on S137A than T115A suggests that AKT signaling may contribute more to YBX2 stabilization than AMPK signaling. Furthermore, we ectopically expressed YBX2 WT and phosphomimic mutants (T115D and S137D) in HEK293T cells followed by treating the cells with compound C or Akt inhibitor VIII. T115D was resistant to compound C-mediated decrease in the protein level, and the S137D level was insensitive to Akt inhibitor (Figures S4A and S4B). In summary, these data suggest phosphorylation of T115 by AMPK or phosphorylation of S137 by Akt2 increases YBX2 protein stability through reducing the ubiquitination-mediated protein degradation.

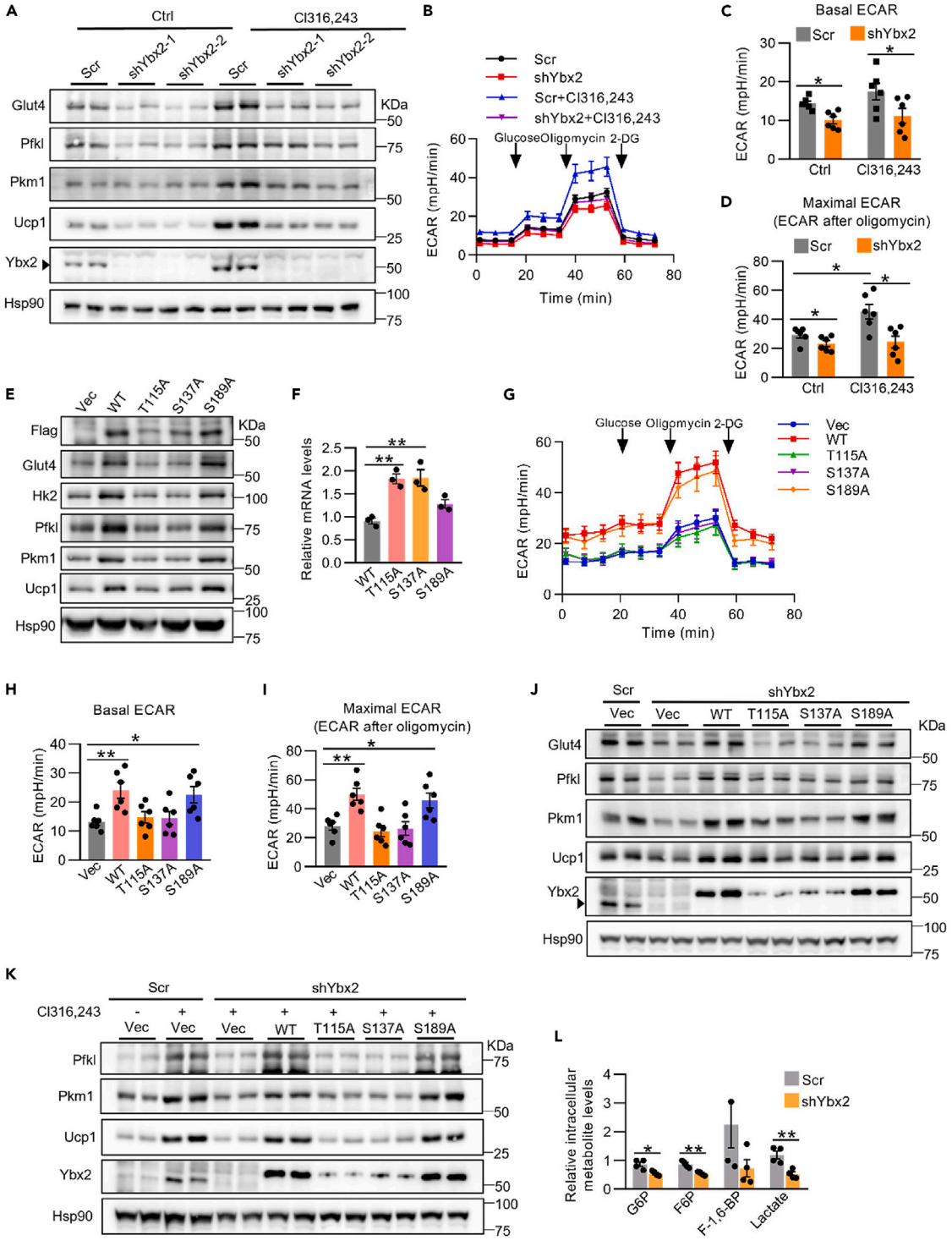

Figure 5. YBX2 regulates glycolysis gene expression in brown adipocytes

(A) Immunoblot analysis for the indicated proteins in brown fat cells. Preadipocytes were infected by lentiviral shRNA targeting *Ybx2*, followed by differentiation to mature adipocytes. Then cells were treated with or without 10 μM Cl316,243 for 14 h.

(B–D) ECAR was measured by Seahorse analyzer with cells treated as in (A) (n = 6). Basal ECAR (C) and maximal ECAR (D) were quantified (n = 6).

(E and F) Preadipocytes bearing lentiviral *Flag-Ybx2* differentiated to mature adipocytes. Immunoblot analysis for the indicated proteins (E) and the measurement of *Ybx2* mRNA level (F) were performed on day 6.

(G–I) ECAR was measure by Seahorse analyzer with cells generated as in (E) (n = 6). Basal ECAR (H) and maximal ECAR (I) were quantified (n = 6).

Figure 5. *Continued*

(J and K) The WT or mutant YBX2 was introduced into YBX2 knockdown adipocytes by lentiviral transduction. Cl316,243 treated the mature adipocytes for 14 h before harvesting the cells (K). The indicated proteins were detected by western blots.

(L) The relative glycolysis metabolite levels were determined by LC-MS/MS in mature brown adipocytes treated by Cl316,243 for 12 h (n = 4 independent samples). Data are expressed as mean ± SEM of biologically independent samples. *p < 0.05, **p < 0.01 by two-way ANOVA (for C, D), by two-tailed unpaired Student's *t* test (for L) or by one-way ANOVA (for F, H, I). See also Figure S5.

YBX2 promotes glycolysis in brown adipocytes *in vivo* or *in vitro*

Next, we explored the biological and physiological importance of the responsiveness of YBX2 to cold stress. Acute cold exposure triggers non-shivering thermogenic program, lipolysis and glycolysis in BAT.[13,14] YBX2 was reported to attach to the lactate dehydrogenase (*Ldhc*) mRNA in mice testes.[8] The *Pkm* (Pyruvate kinase, muscle) gene coding a key enzyme of glycolysis possesses two YBX2 recognition sequence on its promoter.[15] We hypothesize that besides thermogenic activation by stabilizing *Pgc1α* mRNA,[6] YBX2 takes part in the regulation on glucose metabolism in brown adipocytes. To avoid complete loss of *Ybx2* preventing adipocyte differentiation *in vitro*, we knocked down *Ybx2* by 50–70% from preadipocytes which would not affect adipocyte lipogenesis and differentiation.[6] As shown in Figure S5A–C, the knockdown cells differentiated as well as the control, and they expressed similar levels of common fat genes (*Pparγ* and *Fabp4*) and lipogenesis gene (*Acaca*, *Fasn*, *Dgat2*). However, reduced *Ybx2* expression resulted in obviously decreased protein levels of glucose transporter 4 (GLUT4) and phosphofructokinase (PFKL) (Figure 5A). More dramatic suppression on the protein levels of glycolysis enzymes was observed when cells were treated with Cl316,243 for 12 h aiming to activate AMPK and Akt2 kinase. As shown in Figure 5A, βAR activation largely increased levels of glycolytic proteins, however, YBX2 deficiency diminished all these increases. Correspondingly, the basal and maximal extracellular acidification rate (ECAR) that reflects glycolytic activity showed the consistent alteration (Figures 5B–5D). By directly measuring the amount of glucose and lactate in the culture medium, we further verified that ablation of *Ybx2* lessened glucose utilization and lactate production (Figures S5D and S5E).

On the other hand, ectopic expression of WT YBX2 increased the protein, but not mRNA, levels of glucose transporter and glycolytic genes (Figures S5F-S5H). T115A and S137A bore compromised capability to induce glycolytic gene expression and had lower levels of ECAR (Figures 5E–5I). The inability to stimulate downstream gene expression by T115A and S137A was exhibited more noticeably when introducing them into the *shYbx2* adipocytes. As shown in Figures 5J and 5K, exogenous WT and S189A fully recovered the levels of GLUT4, PFKL, and PKM1 in the knockdown cells. T115A and S137A failed to do so, although all the YBX2 constructs expressed at similar mRNA levels (Figures S5I and S5J). The data here provide strong evidence that phosphorylation of YBX2 affects its physiological role in brown adipocytes.

To further confirm the involvement of YBX2 in glycolysis, we employed metabolomics analysis targeted energy metabolism. The *Ybx2*-knockdown adipocytes were treated with Cl316,243 for 12 h followed by metabolite analysis. The levels of the intermediate metabolites of glycolysis, including glucose-6-phosphate (G6P), fructose-6-phosphate (F6P), and lactate, were decreased by nearly 50% (Figure 5L). Additionally, the metabolites of TCA cycle, such as acetyl-CoA, oxaloacetate, α-ketoglutarate, succinate, fumarate, and malic acid, were also significantly declined in *Ybx2*-knockdown cells (Figure S5K), indicating depletion of YBX2 has profound impact on energy metabolism.

Then, we investigate whether loss of YBX2 *in vivo* causes glycolysis defect in BAT. The increased protein level of glycolytic enzymes can be observed after cold exposure or Cl316,243 injection for 3 days (Figures S6A and S6B). We knocked down the *Ybx2* expression by injecting the sh*Ybx2* or control adenovirus into mice BAT, followed by 4°C cold exposure or Cl316,243 injection for 3 days (Figure 6A). The rectal temperature of *Ybx2* knockdown mice was significantly lower than the control group in the first 4-h cold challenge (Figure S6C), which was consistent with the cold intolerance observed in systemic *Ybx2* knockout mice.[6] After cold exposure for 3 days, the BAT with *Ybx2* knockdown expressed less GLUT4, PKM1 and had less metabolites including lactate, ATP, oxaloacetate, and α-ketoglutarate (Figures 6B–6D). Imaging with positron emission tomography-computed tomography (PET-CT) disclosed an obvious decrease in ^{18}fluorodeoxyglucose ([^{18}F]-FDG) uptake by BAT in *Ybx2* knockdown mice after Cl316,243 stimulation (Figures 6E and 6F). Similarly, diminished *Ybx2* reduced lactate production (Figure 6G), and mitigated GLUT4 and PKM1 protein levels without any alteration in their mRNA levels after Cl316,243 treatment (Figures S6D and S6E). Collectively, these data indicated depletion of *Ybx2 in vitro* and *in vivo* suppressed glycolysis by decreasing the expression of glycolytic enzymes, particularly upon β-adrenergic stimuli.

YBX2 promotes translation of glycolytic genes in brown adipocytes

YBX2 is an evolutionarily conserved RNA- and DNA-binding protein that recognizes and associates with Y-box recognition sequence (YRS) (NNCAYCN, where Y is C or U) present in the gene.[16] The RNA immunoprecipitation assay revealed that YBX2 bound to the 5′-UTRs on *Pkm1*, *Hk2*, *Pfkl*, and *Glut4* mRNAs (*Pgc1α* and *Ucp1* genes served as a positive and negative control, respectively). By contrast, the YBX2 Y107A/Y109A mutant (Mu) that lacked the RNA-binding ability failed to associate with glycolytic gene mRNA (Figures 7A and 7B; S7A-S7D).[17] Moreover, the Y107A/Y109A mutant was unable to induce the GLUT4 and PKM1 protein expression, nor was the increase in cell oxygen consumption, glucose utilization, and lactate production (Figures 7C–7F). Meanwhile the GLUT4, HK2, PFKL, and PKM1 expression could be fully restored by reconstitution of WT YBX2 in *Ybx2* knockdown cells, but not by the Y107A/Y109A (Figures 7G and 7H).

Then, we determined how YBX2 modulated the expression of glycolytic genes by binding to their 5′-UTR regions. Knocking down *Ybx2* did not affect glycolytic genes' mRNA stability (Figure S7E). The distribution ratio of these mRNAs in cytoplasm to nuclei was not influenced by YBX2 deficiency either (Figures S7F and S7G). Messenger RNA 5′-UTRs serve as the entry point for the ribosome during translation initiation, thus YBX2 might affect glycolytic gene translation efficiency. We probed the synthesis of nascent proteins upon *Ybx2* depletion by a Click-iT

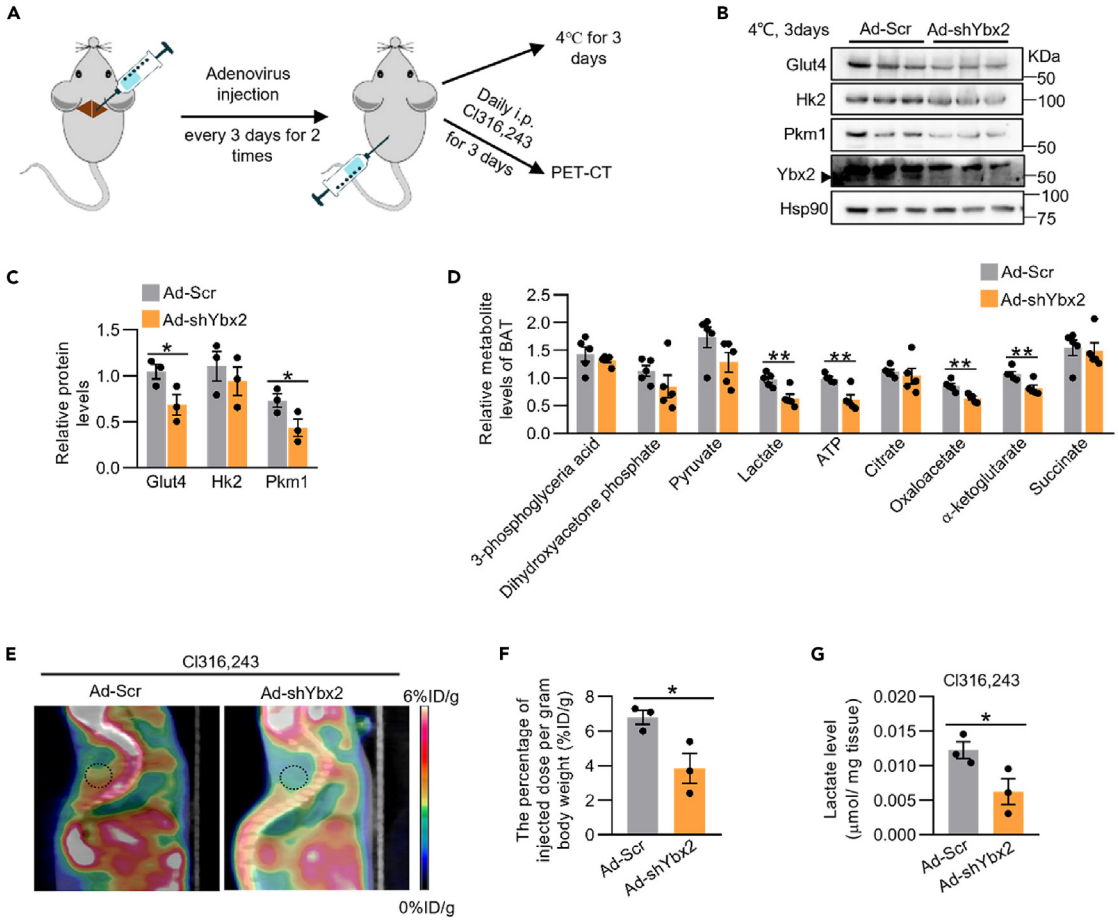

Figure 6. Knockdown of *Ybx2* in BAT suppresses glycolysis *in vivo*

(A) Adenovirus expressing sh*Ybx2* or scrambled control were locally injected into BAT of C57BL/6J mice for twice. One group of mice were housed at 4°C for 3 days. The other group of mice were intraperitoneally injected Cl316,243 (0.5ug/g body weight) daily for 3 days followed by PET-CT scan.

(B and C) The protein levels of glycolytic enzymes in *Ybx2* knockdown BAT after mice were kept at 4°C for 3 days. Protein quantification was performed in (C) (n = 3 each group).

(D) The levels of glycolysis and TCA intermediate metabolites were measured in BAT. Mice were treated as in (A) and exposed to 4°C for 3 days before the metabolite analysis (n = 5 each group).

(E and F) The *Ybx2* knockdown mice were injected with Cl316,243 for 3 days following PET-CT assessing the [^{18}F]-FDG uptake. Representative PET-CT image (E) and quantifications of [^{18}F]-FDG uptake based on the percentage of injected dose per gram of body weight (F) was shown (n = 3 each group). Black circles in (E) showed the area of BAT.

(G) Lactate level in BAT from mice in (E) (n = 3 each group). Data are shown as mean ± SEM of biologically independent samples. *p < 0.05, ***p < 0.01 by Student's *t* test (for C, D, F, G). See also Figure S6.

AHA (azidohomoalanine) labeling assay. Figure 7I demonstrated that newly synthesized HK2, PFKL, and PKM proteins were reduced in *Ybx2*-knockdown cells in the presence or absence of Cl316,234, suggesting reduction in glycolytic gene translation at least is one of the reasons for the decrease in glycolytic enzymes.

DISCUSSION

The phosphorylation modification of proteins is a common and efficient way for cells to adapt to various cellular conditions. Protein phosphorylation propagates signals, changes individual protein functions or stability. Phosphorylation of YBX2 was observed in male germ cells and oocytes by an unknown kinase and increased its affinity to target RNAs.[18,19] In this manuscript, we found that phosphorylated YBX2 by AMPK or Akt increased its protein stability and further facilitated glycolysis in response to β-adrenergic signaling. Adipocyte AMPK is activated responding to exercise as well as caloric restriction,[20,21] and both exercise or caloric restriction promote adipocyte thermogenesis.[22,23] It is possible that phosphorylated YBX2 by AMPK participates in the exercise and caloric restriction-induced adaptive thermogenesis and glycolysis as well.

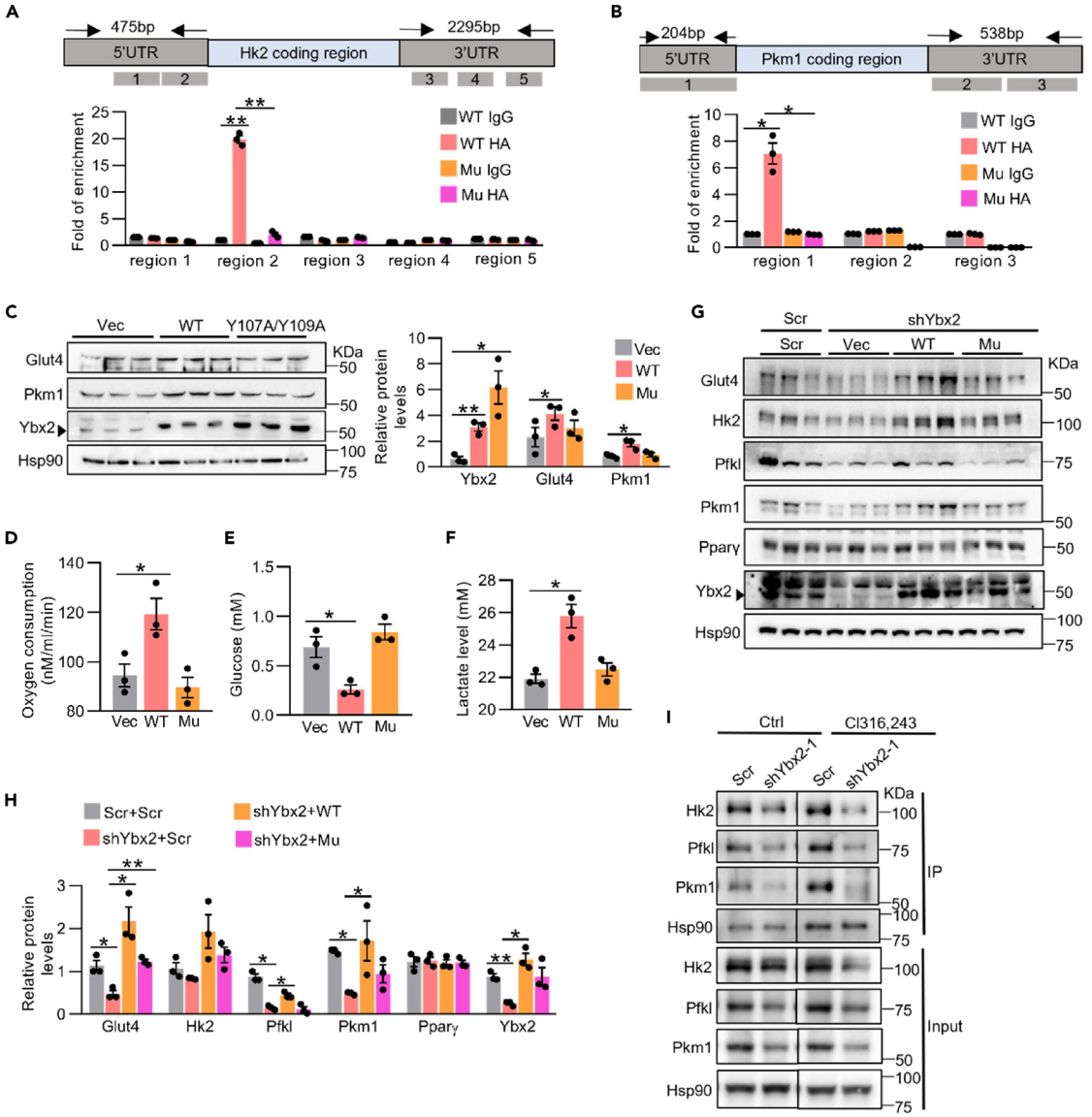

Figure 7. YBX2 enhances translation of glycolytic genes in brown adipocytes

(A and B) RNA immunoprecipitation followed by real-time PCR to detect YBX2 association with *Hk2* (A) and *Pkm1* (B) mRNAs. Brown adipocytes expressing HA-YBX2 were subjected to IgG or HA antibody pulldown. The primers used were indicated. n = 3 independent experiments.

(C) Immunoblot analysis (left) and protein quantification (right) in brown adipocytes for the indicated proteins. Preadipocytes were infected by lentivirus expressing WT or Y107A/Y109A mutant (Mu) *Ybx2*, followed by differentiation induction. n = 3 individual cultures.

(D–F) Oxygen consumption rate (D), glucose (E) and lactate levels (F) in culture media of adipocytes in (C) (n = 3 individual cultures).

(G and H) Immunoblot analysis (G) and protein quantification (H) for indicated genes in brown adipocytes. The YBX2 protein level in knockdown adipocytes was reconstituted by lentiviral expressing WT or Mu *Ybx2* on day 2. n = 3 individual cultures.

(I) A Click-iT AHA labeling assay was used to detect newly synthesized glycolytic protein in *Ybx2* knockdown brown adipocytes on day 4. The adipocytes were treated with or without Cl316,243 for 14 h before the incubation with AHA for 4 h. The experiment was repeated for three times and the representative images were shown. Data are shown as mean ± SEM of biologically independent samples. *p < 0.05, **p < 0.01 by one-way ANOVA. See also Figure S7.

Adaptive thermogenesis incorporates highly activated lipid and glucose metabolism with uncoupling respiration. During cold exposure, large amounts of glucose are taken up and catabolized by BAT to fuel thermogenesis or feed *de novo* lipogenesis, accompanied by increased expression and activities of glycolytic enzymes.[24,25] The catalytic activities of HK and PFK can be activated by AKT or AMPK.[26,27] HIF1α promotes transcription of key glycolytic enzymes to enlarge glycolytic capacity in BAT.[28] AIFM2 supports robust glycolysis by maintaining a high cytosolic NAD^+/NADPH ratio.[29] The innate immune transcription factor IRF3 reduces glycolytic enzyme activities by ISG15-mediated ISGylation covalent modification in adipocytes.[30] Herein, the AMPK/AKT-YBX2-mediated translation regulation represents a new mechanism for

glycolysis control in BAT. Besides modulating glycolysis, YBX2 was reported to stabilize *Pgc1α* mRNA to boost thermogenesis and mitochondrial oxidation.[6] Thus, the defects observed in brown adipocytes or mice with a knockdown of *Ybx2*, for example the lower UCP1 level, decrease in TCA metabolites and lower rectal temperature upon cold stress, should be attributed to both the decreased glycolysis and the reduced PGC1α level. Therefore, YBX2 integrates glycolysis, mitochondrial oxidation, and adaptive thermogenesis together in BAT in response to cold stress.

In prokaryotes some CSD-containing proteins are induced by cold shock and function as RNA-chaperones to stimulate translation of certain mRNAs.[31,32] During spermatogenesis, YBX2 binds to mRNAs to inhibit translation at round spermatid stage.[7,33] When these YBX2-masked mRNAs are required for spermatogenesis, poly(A) binding protein interacting protein 1 (PAIP1) interacts with YBX2 to recruit eukaryotic initiation factor EIF4A reinitiating translation.[8] While how YBX2 enhances glycolytic gene translation in adipocytes remains unknown, which is worth exploring further.

In summary, YBX2 is at the crossroads of thermogenic and glycolytic regulation in brown adipocytes. Our findings broaden the current appreciation of the modulation of YBX2 and help us better understand the physiology of glucose metabolism regulation in brown adipocytes.

Limitations of the study

In this study, we identified the phosphorylated residues responsible for YBX2 protein stabilization in response to adrenergic stimulation. However, the physiological role of YBX2 phosphorylation *in vivo* was not determined. Generating T115A or S137A knockin mutant mice may provide a useful model to fulfill the task. Furthermore, the YBX2 phosphorylation on T115 and S137 has not been verified in human cells or tissues. It is warrant to investigate whether genetic polymorphisms on the corresponding T115 and S137 coding region occurs to human genome and its implication in human diseases.

STAR★METHODS

Detailed methods are provided in the online version of this paper and include the following:

- KEY RESOURCES TABLE
- RESOURCE AVAILABILITY
  - Lead contact
  - Materials availability
  - Data and code availability
- EXPERIMENTAL MODEL AND STUDY PARTICIPANT DETAILS
  - Cell lines
  - Animal studies
- METHOD DETAILS
  - Plasmids and viruses
  - Extracellular acidification rate (ECAR) assay
  - Oxygen consumption assays
  - Lactate and glucose content in culture media
  - *in vivo* adenovirus injection into BAT
  - Metabolomics
  - RNA preparation and quantitative real-time PCR
  - Oil red O staining
  - Western blot and co-immunoprecipitation
  - Cycloheximide chase assay
  - Recombinant protein purification
  - *in vitro* kinase assay
  - Phosphorylation site analysis of YBX2 protein by LC-MS/MS
  - RNA decay analysis
  - RNA subcellular fractionation
  - RNA pull-down
  - AHA metabolic labeling for nascent protein synthesis
- QUANTIFICATION AND STATISTICAL ANALYSIS
  - Statistics

SUPPLEMENTAL INFORMATION

Supplemental information can be found online at https://doi.org/10.1016/j.isci.2023.108091.

ACKNOWLEDGMENTS

This work was supported by grants from National Natural Science Foundation of China (32171140, 31970710 to D.P), Program of Shanghai Academic Research Leader (22XD1400500 to D.P.), China Postdoctoral Science Foundation (2020M680053 to Q.Z), Zhejiang Provincial Natural Science Foundation of China (LQ23C070004 to Q.Z).

AUTHOR CONTRIBUTIONS

Q.Z., C.Y. performed the experiments and acquired data. Q.Z. wrote the original draft of manuscript. X.X. constructed and packaged adenovirus used in this study. W.J. generated YBX2 mutant constructs. Z.Z. analyzed YBX2 mutants half-life time. H.H. provided important reagents for the experiments. D.P. and Y.G. designed the project, supervised the study and modified the manuscript. All the authors discussed the results and commented on the manuscript.

DECLARATION OF INTERESTS

The authors declare no competing conflicts of interest.

Received: May 5, 2023
Revised: August 24, 2023
Accepted: September 26, 2023
Published: September 28, 2023

REFERENCES

1. Wang, W., and Seale, P. (2016). Control of brown and beige fat development. Nat. Rev. Mol. Cell Biol. *17*, 691–702.
2. Kajimura, S., Spiegelman, B.M., and Seale, P. (2015). Brown and beige fat: physiological roles beyond heat generation. Cell Metab. *22*, 546–559.
3. Kazak, L., Chouchani, E.T., Jedrychowski, M.P., Erickson, B.K., Shinoda, K., Cohen, P., Vetrivelan, R., Lu, G.Z., Laznik-Bogoslavski, D., Hasenfuss, S.C., et al. (2015). A creatine-driven substrate cycle enhances energy expenditure and thermogenesis in beige fat. Cell *163*, 643–655.
4. Chen, Y., Ikeda, K., Yoneshiro, T., Scaramozza, A., Tajima, K., Wang, Q., Kim, K., Shinoda, K., Sponton, C.H., Brown, Z., et al. (2019). Thermal stress induces glycolytic beige fat formation via a myogenic state. Nature *565*, 180–185.
5. Ikeda, K., Kang, Q., Yoneshiro, T., Camporez, J.P., Maki, H., Homma, M., Shinoda, K., Chen, Y., Lu, X., Maretich, P., et al. (2017). UCP1-independent signaling involving SERCA2b-mediated calcium cycling regulates beige fat thermogenesis and systemic glucose homeostasis. Nat. Med. *23*, 1454–1465.
6. Xu, D., Xu, S., Kyaw, A.M.M., Lim, Y.C., Chia, S.Y., Chee Siang, D.T., Alvarez-Dominguez, J.R., Chen, P., Leow, M.K.-S., and Sun, L. (2017). RNA Binding Protein Ybx2 Regulates RNA Stability During Cold-Induced Brown Fat Activation. Diabetes *66*, 2987–3000. https://doi.org/10.2337/db17-0655.
7. Cullinane, D.L., Chowdhury, T.A., and Kleene, K.C. (2015). Mechanisms of translational repression of the Smcp mRNA in round spermatids. Reproduction *149*, 43–54. https://doi.org/10.1530/REP-14-0394.
8. He, Y., Lin, Y., Zhu, Y., Ping, P., Wang, G., and Sun, F. (2019). Murine PAIP1 stimulates translation of spermiogenic mRNAs stored by YBX2 via its interaction with YBX2. Biol. Reprod. *100*, 561–572. https://doi.org/10.1093/biolre/ioy213.
9. Pan, D., Huang, L., Zhu, L.J., Zou, T., Ou, J., Zhou, W., and Wang, Y.-X. (2015). Jmjd3-mediated H3K27me3 dynamics orchestrate brown fat development and regulate white fat plasticity. Dev. Cell *35*, 568–583.
10. Tabuchi, C., and Sul, H.S. (2021). Signaling pathways regulating thermogenesis. Front. Endocrinol. *12*, 698619.
11. Calleja, V., Laguerre, M., Parker, P.J., and Larijani, B. (2009). Role of a novel PH-kinase domain interface in PKB/Akt regulation: structural mechanism for allosteric inhibition. PLoS Biol. *7*, e17. https://doi.org/10.1371/journal.pbio.1000017.
12. Evdokimova, V., Ruzanov, P., Anglesio, M.S., Sorokin, A.V., Ovchinnikov, L.P., Buckley, J., Triche, T.J., Sonenberg, N., and Sorensen, P.H.B. (2006). Akt-mediated YB-1 phosphorylation activates translation of silent mRNA species. Mol. Cell Biol. *26*, 277–292.
13. Jung, S.M., Doxsey, W.G., Le, J., Haley, J.A., Mazuecos, L., Luciano, A.K., Li, H., Jang, C., and Guertin, D.A. (2021). In vivo isotope tracing reveals the versatility of glucose as a brown adipose tissue substrate. Cell Rep. *36*, 109459. https://doi.org/10.1016/j.celrep.2021.109459.
14. Blondin, D.P., Frisch, F., Phoenix, S., Guérin, B., Turcotte, É.E., Haman, F., Richard, D., and Carpentier, A.C. (2017). Inhibition of intracellular triglyceride lipolysis suppresses cold-induced brown adipose tissue metabolism and increases shivering in humans. Cell Metab. *25*, 438–447.
15. Yang, J., Medvedev, S., Reddi, P.P., Schultz, R.M., and Hecht, N.B. (2005). The DNA/RNA-binding protein MSY2 marks specific transcripts for cytoplasmic storage in mouse male germ cells. Proc. Natl. Acad. Sci. USA *102*, 1513–1518. https://doi.org/10.1073/pnas.0404685102.
16. Kleene, K.C. (2016). Position-dependent interactions of Y-box protein 2 (YBX2) with mRNA enable mRNA storage in round spermatids by repressing mRNA translation and blocking translation-dependent mRNA decay. Mol. Reprod. Dev. *83*, 190–207. https://doi.org/10.1002/mrd.22616.
17. Bouvet, P., Matsumoto, K., and Wolffe, A.P. (1995). Sequence-specific RNA recognition by the Xenopus Y-box proteins. An essential role for the cold shock domain. J. Biol. Chem. *270*, 28297–28303.
18. Herbert, T.P., and Hecht, N.B. (1999). The mouse Y-box protein, MSY2, is associated with a kinase on non-polysomal mouse testicular mRNAs. Nucleic Acids Res. *27*, 1747–1753. https://doi.org/10.1093/nar/27.7.1747.
19. Yu, J., Hecht, N.B., and Schultz, R.M. (2001). Expression of MSY2 in mouse oocytes and preimplantation embryos. Biol. Reprod. *65*, 1260–1270. https://doi.org/10.1095/biolreprod65.4.1260.
20. Park, H., Kaushik, V.K., Constant, S., Prentki, M., Przybytkowski, E., Ruderman, N.B., and Saha, A.K. (2002). Coordinate regulation of malonyl-CoA decarboxylase, sn-glycerol-3-phosphate acyltransferase, and acetyl-CoA carboxylase by AMP-activated protein kinase in rat tissues in response to exercise. J. Biol. Chem. *277*, 32571–32577. https://doi.org/10.1074/jbc.M201692200.
21. Vega-Martín, E., González-Blázquez, R., Manzano-Lista, F.J., Martín-Ramos, M., García-Prieto, C.F., Viana, M., Rubio, M.A., Calle-Pascual, A.L., Lionetti, L., Somoza, B., et al. (2020). Impact of caloric restriction on AMPK and endoplasmic reticulum stress in peripheral tissues and circulating peripheral blood mononuclear cells from Zucker rats. J. Nutr. Biochem. *78*, 108342. https://doi.org/10.1016/j.jnutbio.2020.108342.
22. Vidal, P., and Stanford, K.I. (2020). Exercise-Induced Adaptations to Adipose Tissue Thermogenesis. Front. Endocrinol. *11*, 270. https://doi.org/10.3389/fendo.2020.00270.
23. Zhang, S., Sun, S., Wei, X., Zhang, M., Chen, Y., Mao, X., Chen, G., and Liu, C. (2022). Short-term moderate caloric restriction in a high-fat diet alleviates obesity via AMPK/SIRT1 signaling in white adipocytes and liver. Food Nutr. Res. *66*. https://doi.org/10.29219/fnr.v66.7909.
24. Bartelt, A., Bruns, O.T., Reimer, R., Hohenberg, H., Ittrich, H., Peldschus, K., Kaul, M.G., Tromsdorf, U.I., Weller, H., Waurisch, C., et al. (2011). Brown adipose tissue activity

controls triglyceride clearance. Nat. Med. *17*, 200–205. https://doi.org/10.1038/nm.2297.

25. Orava, J., Nuutila, P., Lidell, M.E., Oikonen, V., Noponen, T., Viljanen, T., Scheinin, M., Taittonen, M., Niemi, T., Enerbäck, S., and Virtanen, K.A. (2011). Different metabolic responses of human brown adipose tissue to activation by cold and insulin. Cell Metab. *14*, 272–279. https://doi.org/10.1016/j.cmet.2011.06.012.
26. Doménech, E., Maestre, C., Esteban-Martínez, L., Partida, D., Pascual, R., Fernández-Miranda, G., Seco, E., Campos-Olivas, R., Pérez, M., Megias, D., et al. (2015). AMPK and PFKFB3 mediate glycolysis and survival in response to mitophagy during mitotic arrest. Nat. Cell Biol. *17*, 1304–1316. https://doi.org/10.1038/ncb3231.
27. Bando, H., Atsumi, T., Nishio, T., Niwa, H., Mishima, S., Shimizu, C., Yoshioka, N., Bucala, R., and Koike, T. (2005). Phosphorylation of the 6-phosphofructo-2-kinase/fructose 2,6-bisphosphatase/PFKFB3 family of glycolytic regulators in human cancer. Clin. Cancer Res. *11*, 5784–5792. https://doi.org/10.1158/1078-0432.ccr-05-0149.
28. Basse, A.L., Isidor, M.S., Winther, S., Skjoldborg, N.B., Murholm, M., Andersen, E.S., Pedersen, S.B., Wolfrum, C., Quistorff, B., and Hansen, J.B. (2017). Regulation of glycolysis in brown adipocytes by HIF-1α. Sci. Rep. *7*, 4052. https://doi.org/10.1038/s41598-017-04246-y.
29. Nguyen, H.P., Yi, D., Lin, F., Viscarra, J.A., Tabuchi, C., Ngo, K., Shin, G., Lee, A.Y.-F., Wang, Y., and Sul, H.S. (2020). Aifm2, a NADH Oxidase, Supports Robust Glycolysis and Is Required for Cold- and Diet-Induced Thermogenesis. Mol. Cell *77*, 600–617.e4. https://doi.org/10.1016/j.molcel.2019.12.002.
30. Yan, S., Kumari, M., Xiao, H., Jacobs, C., Kochumon, S., Jedrychowski, M., Chouchani, E., Ahmad, R., and Rosen, E.D. (2021). IRF3 reduces adipose thermogenesis via ISG15-mediated reprogramming of glycolysis. J. Clin. Invest. *131*, e144888. https://doi.org/10.1172/JCI144888.
31. Graumann, P.L., and Marahiel, M.A. (1998). A superfamily of proteins that contain the cold-shock domain. Trends Biochem. Sci. *23*, 286–290.
32. Jiang, W., Hou, Y., and Inouye, M. (1997). CspA, the major cold-shock protein of Escherichia coli, is an RNA chaperone. J. Biol. Chem. *272*, 196–202.
33. Yang, J., Medvedev, S., Reddi, P.P., Schultz, R.M., and Hecht, N.B. (2005). The DNA/RNA-binding protein MSY2 marks specific transcripts for cytoplasmic storage in mouse male germ cells. Proc. Natl. Acad. Sci. USA *102*, 1513–1518.
34. Pan, D., Fujimoto, M., Lopes, A., and Wang, Y.-X. (2009). Twist-1 is a PPARdelta-inducible, negative-feedback regulator of PGC-1alpha in brown fat metabolism. Cell *137*, 73–86. https://doi.org/10.1016/j.cell.2009.01.051.

STAR★METHODS

KEY RESOURCES TABLE

REAGENT or RESOURCE	SOURCE	IDENTIFIER
Antibodies		
Anti-Ucp1	Abcam	Cat#ab10983; RRID:AB_2241462
Anti-Ucp1	Alpha Diagnostic International	Cat#UCP11-A; RRID:AB_1624298
Antl-H4	Abcam	Cat#ab177840; RRID:AB_2650469
Anti-Ybx2	Abcam	Cat#ab154829; RRID:AB_2749836
Anti-Hsp90	Proteintech	Cat#13171-1-AP; RRID:AB_2120924
Anti-Fabp4	Proteintech	Cat#12802-1-AP; RRID:AB_2102442
Anti-Flag	Proteintech	Cat#20543-1-AP; RRID:AB_11232216
Anti-Gst	Proteintech	Cat#66001-1-Ig; RRID:AB_10951482
Anti-α-Tubulin	Proteintech	Cat#66031-1-Ig; RRID:AB_11042766
Anti-Glut1	Proteintech	Cat#21829-1-AP; RRID:AB_10837075
Anti-Pkm1	Proteintech	Cat#15821-1-AP; RRID:AB_2163820
Anti-Pfkl	Proteintech	Cat#15652-1-AP; RRID:AB_2162873
Anti-Hk2	Proteintech	Cat#22029-1-AP; RRID:AB_11182717
Anti-Akt2	Proteintech	Cat#17609-1-AP; RRID:AB_2305350
Anti-HA	Proteintech	Cat#51064-2-AP; RRID:AB_11042321
Anti-AMPKα	Cell Signaling Technology	Cat#5831; RRID:AB_10622186
Anti-phospho-AMPKα Thr172	Cell Signaling Technology	Cat#2535; RRID:AB_331250
Anti-phospho-PKA substrate	Cell Signaling Technology	Cat#9624; RRID:AB_331817
Anti-Pparγ 1/2	Cell Signaling Technology	Cat#2443; RRID:AB_823598
Anti-Glut4	Cell Signaling Technology	Cat#G4048; RRID:AB_1840900
Anti-phospho-(Ser/Thr) AMPK substrate motif (LXRXXpS/pT)	Cell Signaling Technology	Cat#5759; RRID:AB_10949320
Anti-p-Akt2	Absci	Cat#ab11124
Anti-HA	Santa Cruz Biotechnology	Cat#sc-805; RRID:AB_631618
Anti-IgG	Sigma	Cat#I5006; RRID:AB_1163659
Anti-Mouse HRP	YEASEN Biotech	Cat#33201ES60; RRID:AB_10015289
Anti-Rabbit HRP	YEASEN Biotech	Cat#33101ES60
Chemicals, peptides, and recombinant proteins		
Fetal bovine serum	HyClone	SH30393.03
ChamQ Universal SYBR Qpcr Master Mix	Vazyme	Q711
RNA isolater Total RNA Extraction Reagent	Vazyme	R401
EZ Trans Cell Transfect Regents	Life-iLab	AC04L092
H-89 dihydrochloride hydrate	Meilunbio	MB5403
MG132	Meilunbio	MB5137
High-glucose Dulbecco's modified Eagle medium	Meilunbio	MA0212
Compound C	Meilunbio	MB7217
Akt inhibitor VIII	Meilunbio	MB4288
AMPKα1β1γ1 Kinase Enzyme System	Promega	V1921
Insulin	Sigma-Aldrich	I3536
T3	Sigma-Aldrich	T2877
IBMX	Sigma-Aldrich	I5859
Indomethacin	Sigma-Aldrich	I7378

(*Continued on next page*)

Continued

REAGENT or RESOURCE	SOURCE	IDENTIFIER
Dexamethasone	Sigma-Aldrich	D4902
Glucose	Sigma-Aldrich	G7021
CI316,243 disodium salt	Tocris Bioscience	1499
Actinomycin D	MCE	HY-17559
Oligomycin	MCE	HY-N6782
2-DG	MCE	HY-13966
A-769662	MCE	HY-50662
Seahorse XFe96/XF Pro FluxPak Mini	Agilent	103793
Seahorse XF Calibrant Solution	Agilent	103793
Seahorse XF 200 mM glutamine solution	Agilent	103579
Seahorse XF DMEM	Agilent	103575
L-azidohomoalanine	Invitrogen	C10102
Protein A sepharose	GE Healthcare	17-0780-01
High fat diet (HFD) (60 kcal% fat)	Research Diets, Inc	D12492
Critical commercial assays		
Click-iT Protein Reaction Buffer Kit	Invitrogen	C10276
Lactic Acid assay kit	Nanjing Jiancheng Bioengineering Institute	A-019-2-1
Glucose assay kit	Applygen	E1010
The nuclear and cytoplasmic protein extraction kit	Beyotime	P0027
Experimental models: Cell lines		
HEK293T	ATCC	CRL-3216; RRID: CVCL_0063
Immortalized brown preadipocytes	Generated in-house	N/A
Experimental models: Organisms/strains		
C57BL/6J	Shanghai Model Organisms Center, Inc	RRID:IMSR_JAX:000664
Oligonucleiotides		
Primers used in this study, see Table S3	This paper	N/A
Software and algorithms		
FLIR thermal imaging cameras	FLIR tools	RRID:SCR_016330
Graphpad Prism	GraphPad Software	Version 8; RRID: SCR_002798

RESOURCE AVAILABILITY

Lead contact

Further information and requests for resources and reagents should be directed to and will be fulfilled by the lead contact, Dongning Pan (dongning.pan@fudan.edu.cn).

Materials availability

Plasmids and cell lines generated in this study are available upon request with the lead contact.

Data and code availability

- Data reported in this paper will be shared by the lead contact upon request.
- This paper does not report original code.
- Any additional information required to reanalyze the data reported in this paper is available from the lead contact upon request.

EXPERIMENTAL MODEL AND STUDY PARTICIPANT DETAILS

Cell lines

Immortalized BAT preadipocytes was generated and induced differentiation as described previously.[34] Briefly, at day -2, brown adipocytes at 70% confluent were changed to DMEM supplemented with 10% FBS, 20 nM insulin and 1 nM T3. At day 0, confluent brown adipocytes were induced by DMEM containing 10% FBS, 20 nM insulin, 1 nM T3, 0.5 mM isobutyl-methylxanthine, 0.5 μM dexamethasone, and 0.125 mM indomethacin for 2 days. Then cells were still culturing in DMEM containing 10% FBS, 20 nM insulin and 1nM T3 for another 4 days. At day 6, cells were fully differentiated and harvested.

Animal studies

All studies involving animal experimentation were approved by the Fudan University Shanghai Medical College Animal Care and Use Committee. Male C57BL/6 mice were purchased from the Shanghai Model Organisms Center, Inc. (Shanghai, China). All the mice were maintained on a standard rodent chow diet with 12 h light and dark cycles. For cold challenge experiments, 8-week-old mice were placed in a 4°C cold room for the indicated time. β3-adrenergic agonist CI316,243 was intraperitoneally into mice at 0.5μg/mg body weight for the indicated time. Mice rectal temperature was recorded by an animal electronic thermometer (ALT-ET03, Shanghai Alcott Biotech Co. LTD). For micro-PET/CT experiments, mice were fasted for 4 h and lightly anesthetized. Then each animal was intraperitoneally injected with 100 μCi of ^{18}F-FDG diluted in saline and waited for 1 -h following Micro-PET/CT analysis.

METHOD DETAILS

Plasmids and viruses

Ybx1, *Ybx2*, *Ybx3* and *AMPKα1* short hairpin RNA (shRNA) lentiviral constructs were generated using psp108 vector (Addgene). *Ybx1* shRNA-1 targeting sequence is: 5′-GTATCGCCGAAACTTCAATTA-3′; shRNA-2: 5′- GCGAAGGTTCCCACCTTA.

CTA-3′. *Ybx2* shRNA-1 targeting sequence is: 5′-GCGTCCACGAAACCGTCCCTA.

-3′; shRNA-2: 5′-GTAGGTTCCGGAGGTTCATTC-3′. *Ybx3* shRNA-1 targeting sequence is: 5′- CCAGATGGAGTTCCTGTAGAA-3′; shRNA-2: 5′-GTTCAACGT.

CAGAAATGGATA-3′; *AMPKα1* shRNA-1: 5′- TTGTTGGATTTCCGTAGTATT-3′; shRNA-2: 5′- CACGAGTTGACCGGACATAAA-3′. *Ybx2* shRNA was constructed into adenoviral AdEasy-1 system. Full-length human *Ybx2* cDNA and Ybx2 mutants (Y107A/Y109A, T115A, S137A, S189A, T115A/S137A, and T115A/S137A/S189A) were generated by PCR and confirmed by sequencing. These ORFs were cloned into lentiviral pENTER1A vector (Addgene). For knockdown lentivirus production, psp108 vector along with plasmids pMD2.G (Addgene) and psPAX2 (Addgene) were co-transfected into the HEK293T cells. Overexpressed plasmids and the packing plasmids (pLP1, pLP2, pVSVG) were transfected into the HEK293T cells. The viral supernatant was harvested after 48 h of transfection.

Extracellular acidification rate (ECAR) assay

Brown preadipocytes were differentiated in 12-well plates, and reseeded into a 96-well plate at a density of 8000 cells per well on day 5. Cells were treated with CI316,243 for 14 h on the next day following the ECAR assay using the Seahorse XFe Extracellular Flux Analyzer (Agilent). On the day of experiments, cells were maintained in XF assay medium supplemented with 1 mM glutamine and subjected to glycolysis stress by adding glucose (10 mM), oligomycin (1 μM), and 2-deoxy-D-glucose (2-DG) (50 mM).

Oxygen consumption assays

Cultured brown adipocytes were collected by trypsinization. Then cells were suspended in 1 ml phosphate-buffered saline containing 25 mM glucose, 1 mM sodium pyruvate and 2 % BSA. Respiration was measured with a Clark-type electrode (Oxygraph$^+$ system, Hansatech).

Lactate and glucose content in culture media

Cells were changed into fresh media on day 4. Then media was harvested on day 6 to determine the lactate and glucose content by biochemical assay kits.

in vivo adenovirus injection into BAT

Adenoviruses were purified with cesium chloride ultracentrifugation and virus tilters were determined in HEK293T cells by counting green fluorescent protein (GFP) positive cells. 2-month-old male mice were used for viral injection. 100 μl of each adenovirus (5x10^9 pfu) diluted in phosphate buffer saline was injected bilaterally into the BATs. Mice were injected every 3 days for twice.

Metabolomics

The preadipocytes were infected with sh*Ybx2* lentivirus and induced to mature adipocytes. Then cells were washed twice with phosphate buffer saline, collected, stored at -80°C and prepared for LC-MS/MS (Applied Protein Technology, Shanghai, China). The BATs from control or *Ybx2* knockdown mice were subjected to LC-MS/MS assay in core facility of Institutes of Biomedical Science Fudan University.

RNA preparation and quantitative real-time PCR

Total RNA from the cells and tissues were extracted using TRIzol (Vazyme) and an equal amount of RNA was reverse transcribed by HiScipt® QRT SuperMix with gDNA wiper. Quantitative real-time PCR was following the instruction of chamQ SYBR qPCR Master Mix with ViiA 7 Real-Time PCR system (Applied biosystems). The mRNA level of ectopically expressed *Ybx2* was determined by human *Ybx2*-specific primers. The endogenous *Ybx2* level in mouse adipocytes was analyzed by mouse *Ybx2*-specific primers.

Oil red O staining

Mature adipocytes were washed once by phosphate buffer saline and were fixed in 4% buffered formaldehyde at room temperature. Then cells were stained with Oil Red O working solution for 1 h. Later, cells were washed with MilliQ water for several time and prepared to picture.

Western blot and co-immunoprecipitation

For western blot, the cells or adipose tissues were homogenized in cell lysis buffer (100 mM NaCl, 0.5% Triton-X-100, 5% glycerol, 50 mM Tris-HCl (pH 7.5), 1 mM PMSF and protease inhibitor mixture cocktail). Lysates were collected by centrifugation at 16,000 *g* for 10 minutes at 4°C. Protein concentration was determined using a BCA protein assay kit (YEASEN, 20201ES86). The protein lysates were separated by sodium dodecyl sulfate-polyacrylamide gel electrophoresis (SDS-PAGE) and detected with a chemiluminescence (ECL) system. For detect interaction between YBX2 and AMPKα1 or Akt2, *HA-Ybx2* and *Flag-Akt2* were transfected in HEK293T cells, or lentivirus against *Flag-Ybx2* was overexpressed in brown adipocytes. Total HEK293T or brown adipocytes lysates were collected and incubated with HA-beads or Flag-beads (Smart-Lifesciences, SA068001, SA042001) for 3 h. Then beads were washed for three times with wash buffer. The immunoprecipitates were analyzed by western blot.

Cycloheximide chase assay

To compare YBX2 protein stability of several mutants (WT, T115A, S137A, T115A/S137A), HEK293T cells were transfected above plasmids separately as indicated. After cycloheximide (50 μM) treatment as indicated, cells lysates were separated by SDS-PAGE and YBX2 protein level was detected using HA antibody.

Recombinant protein purification

Full-length human *Ybx2* mutants (WT, T115A, S137A, S189A) or constitutive activated *Akt2* (CA-Akt2) was cloned in pGex4T-1 and expressed in Escherichia coli BL21 following 0.2 mM isopropyl β-D-thiogalactopyranoside for 18 h at 25°C. The recombinant YBX2 or CA-Akt2 protein were purified using glutathione-sepharose beads (Smart-Lifesciences, SA008010), eluted with reductive glutathione, dialyzed against 20 mM Tris-HCl at pH 8.0, and 10 % glycerol, and quantified for protein content by BCA protein assay kit.

in vitro kinase assay

For AMPK kinase assay, GST-YBX2 fusion proteins (2ug) (WT, T115A, S189A) was used for incubation with the commercial AMPKα1/β1/γ1 (100 ng) at 30°C for 30 min. For Akt2 kinase assay, YBX2 recombinants (WT, T115A, S137A) (2 ug) was mixed with CA-Akt2 fusion protein (500 ng) at 30°C for 30 min. The reactions were terminated with SDS loading buffer and subjected to SDS-PAGE. Phosphorylation levels were presented by phospho-AMPK substrate motif (LXRXXpS/pT) antibody or phospho-Akt substrate (RXRXXpS/pT) antibody.

Phosphorylation site analysis of YBX2 protein by LC-MS/MS

YBX2-Flag protein was immunoprecipitated by Flag beads from mature adipocytes after CI316,243 treatment for 12 hr. Purified GST-YBX2 protein was incubated with active AMPKα1/β1/γ1 complex in the presence of ATP, and then separated by SDS-PAGE and depicted with colloidal Coomassie blue staining. Bands of YBX2 were excised, and analyzed by Human Phenome Institute, Fudan University.

RNA decay analysis

Brown preadipocytes were infected with sh*Ybx2* lentivirus, then were induced differentiation for 8 days. The cells were treated with 5 μg/ml actinomycin D to inhibit the synthesis of new mRNAs. Glycolysis gene mRNA level were analyzed by real-time PCR at indicated time.

RNA subcellular fractionation

Differentiated brown adipocytes were lysed with buffer (10 mM HEPES (pH 7.9), 10 mM KCl, 0.1 mM EDTA and proteinase inhibitor) swelled on ice for 15 minutes, and added NP-40 to a final concentration of 0.6%. Cells were then centrifuged at 3,000 *g* for 5 minutes and supernatants were collected as the cytoplasmic fraction. The nuclear pellets were resuspended in 20 mM HEPES (pH 7.9), 0.4 M NaCl, 10% glycerol, 1 mM EDTA and proteinase inhibitor and incubated at 4°C for 30 minutes. Later the nuclear extracts were harvested after centrifuge. For RNA analysis, cytoplasmic and nuclear fraction were extracted using a nuclear and cytoplasmic protein extraction kit according to the manufacturer's instructions. All the buffer above were added with 150 units /ml RNase inhibitor (NEB, M0314) to suppress ribonucleases. RNA was extracted from the nuclear and cytoplasmic fractions as described above.

RNA pull-down

Mature brown adipocytes expressing HA-YBX2 WT or HA-YBX2 Mu (Y107A /Y109A) were irradiated with 254 nm UV-C light at 300 mJ /cm^2 on ice. Cells were harvested and incubated in lysis buffer (50 mM Tris-HCl (pH 7.4), 100 mM NaCl, 1% NP-40, 0.1% SDS, 0.5% sodium deoxycholate, proteinase inhibitor, DNase (Qiagen) and Rnase inhibitor) for 15 min. After centrifuge at 15,000 g at 4°C for 10 min, supernatants were immunoprecipitated with anti-HA antibody (Santa cruz, sc-805X) or anti-IgG (Sigma, I5006) antibody for 8 h and then were rotated with protein A sepharose (GE Healthcare, 17-0780-01) for another 1 h. Antibody-beads were washed twice in high-salt buffer (50 mM Tris-HCl (pH 7.4), 1 M NaCl, 1 mM EDTA, 1% NP-40, 0.1% SDS, 0.5% sodium deoxycholate) and washed in low-salt buffer (10 Mm Tris-HCl (pH 7.4), 10 mM $MgCl_2$, 0.2% Tween-20) for the last time. Later, beads were suspended in buffer (Tris-HCl (pH 8.0), 1% SDS, 1mM $CaCl_2$, 2 ug/ul proteinase K), incubated at 55°C for 30 min, and were added 1 ml TRIzol. RNA was extracted as described above.

AHA metabolic labeling for nascent protein synthesis

Preadipocytes were infected with lentiviruses carrying sh*Ybx2* or control, selected with puromycin, and induced differentiation until day 4. Then cells were cultured in methionine-free medium for 1 h, followed by incubation with 50 μM AHA (L-azidohomoalanine) for 4 h. Cells were harvested, suspended into AHA lysis buffer (1% SDS, 50 mM Tris-HCl (pH 8.0)), sonicated for 30 cycles of 30 s each, and centrifuged for 10 min at 13,000 g at 4 °C. Cell lysates were mixed with Click reaction buffer with 40 μM biotin-alkyne using the Click-iT® Protein Reaction Buffer Kit. Protein components were purified and incubated with Dynabeads M-280 Streptavidin for 3 h at 4°C, followed by washing 3 times with AHA lysis buffer. Finally, SDS-PAGE and immunoblotting were performed for the indicated protein.

QUANTIFICATION AND STATISTICAL ANALYSIS

Statistics

Data are presented as mean ± sem. Statistical analysis was performed using GraphPad Prism v.8.0 (GraphPad software). Statistical significance was determined by using unpaired two-tailed Student's t test for two group comparisons, one-way ANOVA with Dunnett's test or two-way ANOVA with Tukey's test for multiple comparisons. At least three independent cell cultures were used for all *in vitro* analysis. No technical replicates were used.